

# X-Ray Diagnostic Developments in the Perspective of DEMO

D. Pacella<sup>1</sup>, A. Romano<sup>1</sup>, L. Gabellieri<sup>1</sup>, F. Causa<sup>1</sup>, F. Murtas<sup>2</sup>, G. Claps<sup>2</sup>, W. Choe<sup>3</sup>, S.H. Lee<sup>3</sup>, S. Jang<sup>3</sup>, J. Jang<sup>3</sup>, J. Hong<sup>3</sup>, T. Jeon<sup>3</sup>, H. Lee<sup>3</sup>

<sup>1</sup>*Euratom-ENEA Association, C.R. Frascati, Via E. Fermi, 45 - 00044 Frascati, Rome, Italy*

<sup>2</sup>*Istituto Nazionale di Fisica Nucleare, Via E. Fermi 40, 00044 Frascati, Rome Italy*

<sup>3</sup>*Korea Advanced Institute of Science and Technology, 291 Daehak-ro, Yuseong-gu, Daejeon 305-701, Korea*

**Abstract.** Soft X-ray diagnostics at present are not adequate for a burning plasma experiment, neither in term of hardware nor as diagnostic conception. Detectors have to be radiation tolerant, easily shielded, with low sensitivity to neutrons and gammas and with energy discrimination. Layout and viewing capability should be more flexible, thanks to the use also of optical devices, going toward a configuration intermediate between discrete tomography and pure imaging. The general conception of these diagnostics should therefore evolve in the direction of pattern recognition for a real time feedback. This work is focused on the diagnostic developments undertaken at the ENEA- Frascati X-ray Laboratory, following in particular three directions: gas detector for fast and advanced high density tomography, C-MOS solid state imaging detectors for slow control and X-ray polycapillary optics. GEM gas detectors in photon counting mode (noise free) were developed in the range 1-30 keV having high efficiency, high time resolution (up to microseconds), energy discrimination in bands and optical flexibility. Discrimination of X-rays, neutrons and gammas has been demonstrated, thanks to the combination of intrinsic gain and discrimination thresholds, at neutron fluxes ( $10^7$  n/s\*cm<sup>2</sup>) comparable with the expected ones at the ports of ITER. GEM detectors are also extremely flexible in the design, allowing optimization of the measurements and solutions for shielding or minimization of the effect of background radiation. Two solid state C-MOS imagers working in photon counting mode, one based on Si semiconductor (Medipix-2, range 5-30 keV) and the other one having a CdTe sensor (Pixirad, range 2-100 keV) have been characterized in laboratory. C-MOS imagers have features and performances thoroughly complementary to the GEM detector and, thanks to their higher pixel density, could be used as remote imaging detectors coupled to optics. X-ray polycapillary lenses have been therefore studied in the laboratory both as imaging optical device (full lens) or to define a line of sight (cylinder lens); the preliminary results are encouraging toward the goal of using these lenses to transport X-ray radiation far from the reactor. Reflective or diffractive X-ray optics can be also an option for tomography. A GEM detector has been installed at KSTAR and in the next future hopefully the other approaches will be tested there: once their feasibility will be demonstrated, the issue of the improvement of the radiation tolerance will be faced and the development of algorithms for data analysis as well.

**Keywords:** X-ray detector, imaging, tomography and optics. Plasma physics diagnostics.

**PACS:** Replace this text with PACS numbers; choose from this list: <http://www.aip.org/pacs/index.html>

## REQUIREMENTS FOR NEW X-RAY DIAGNOSTICS IN DEMO PERSPECTIVE

In the perspective of DEMO, Soft X ray diagnostics will require strong improvements not only in terms of hardware and software, but even in their own conception and in the philosophy of the measurement. In terms of hardware, detectors have to be immune to neutrons and gammas as much as possible and the electronics should be radiation tolerant as well. In addition, the diagnostic system should be compact and integrated in order to facilitate shielding. In terms of performances, photon counting mode and energy discrimination offer unprecedented advantages. Optical flexibility and the use of X ray optics are also crucial issues. Finally, an important effort should be devoted to the development of conceptual frameworks in which these new X ray diagnostics will be used, taking into account hybrid schemes tomography/imaging, spectral imaging, pattern recognition, fast algorithm to assess physical parameters (impurities, plasma shaping, heating effects) in real time for feedback control and also as a platform for a cluster of X-ray detector, complementary in term of space/time resolution, energy domains and so on.

## DEVELOPMENT OF NEW TECHNOLOGIES IN ENEA C. R. FRASCATI

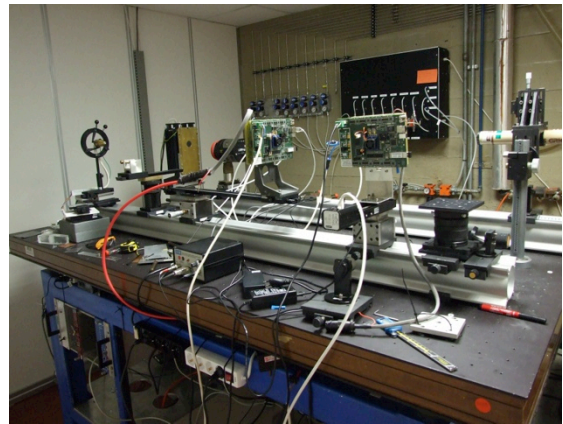
It is nowadays evident that imaging and/or tomographic X-ray diagnostics will take a leading role in future magnetic fusion devices. In addition the advantage and the relevance of energy discrimination capability, although limited to broad energy bands, is meanwhile well established. Moreover harsh environment will be the foreseen bed for all devices in the future of MF diagnostics and the possibility of displacing detectors far from the machine appears a mandatory goal to achieve. Magnetic Fusion Plasma is an extended source, the distance from the source to the detector that should be taken into account is of the order of meters and X-ray emission up to 100 keV is the energy domain of interest. Therefore, a new laboratory equipped and fully shielded to work with Soft and Hard X rays (up to 120 keV) has been built in ENEA-Frascati (Fig. 1). The size of the laboratory allows measurements at large distances (up to 7 m) from X sources, optics and detectors. The laboratory is equipped with X-ray tubes (Moxtek 10-50 kV Bullet and Micro-focus 35-80 kV) that have been absolutely calibrated in house using a Si-PIN diode, SDD diode and a spectroscopic CdTe detector. The laboratory is also equipped for gas and solid state imaging detectors (CCD, Medipix-2 and PIXIRAD). Gas Electron Multiplier detectors, working in photon counting mode and offering imaging capability, can be tested with many different gas mixtures, thanks to the gas fuelling system of the laboratory, digitally controlled with extremely high precision.

A software tool to simulate the photon flux emitted by the X-ray sources and those impinging and/or detected by any detector has been developed and this is a relevant equipment of the facility. All the devices are remotely controlled outside and all the X-ray tubes and sources, imaging detectors, spectrometers and filters are absolutely calibrated. Therefore, any experimental configuration can be simulated, taking into account its absolute spectral response.

In this context, the study of new optical devices, such as the polycapillary lenses (of which promising imaging properties and good resolving power has been already demonstrated) is in progress, because they are able to transport X-ray radiation far from the harsh environment and to preserve the imaging capability. New frontier C-MOS imaging detectors such as Medipix-2 (5-30 keV) and PIXIRAD (2-100 keV) were characterized using these facilities. Their high 2D spatial resolution, in photon counting mode, could represent an attractive feature for application in magnetic fusion experiments, particularly if coupled with X-ray optics.



(a)



(b)

**FIGURE 1.** The facilities at ENEA C. R. Frascati: (a) the newly opened SXR laboratory and (b) the experimental bench for the characterization of sources, detectors and devices.

## SXR IMAGING WITH GEM PINHOLE CAMERA IN HARSH ENVIRONMENTS

A triple GEM detector is a micropatterned gas detector comprising a primary ionization gap, where X-ray photon conversion occurs, three consecutive GEM foils representing the amplification stages, and a 2D printed circuit board with 144 squared pixels where the signal is collected. The detector has an active area of  $10 \times 10 \text{ cm}^2$ , while pixels have dimensions of  $0.8 \times 0.8 \text{ cm}^2$  ( $12 \times 12$  squared pixels). Since it works in photon counting mode and with direct conversion, it offers high sensitivity (detection efficiency up to 0.3), noise free, high dynamic range (6 orders of magnitude) and good time resolution (5 MHz/pixel, continuous framing rate at 1 kHz and up to 100 kHz for limited time windows) [1]. The front-end electronics is integrated in microchips called CARIOCA, developed at CERN, in

groups of 8 channels [2]. The firmware of the motherboard with FPGA, at the rear of the detector, has been developed to include the data acquisition system (DAQ) [3]. Especially for applications in harsh environments, with high radiative background, a triple rather than a single-GEM detector is more appropriate because by lowering the gain in each stage the risk of possible discharges due to the high radiation flux, is minimized.

The Frascati Neutron Generator (FNG) facility, [4], was used to characterize the GEM response under high neutron and gamma irradiation. The facility permits irradiation with 14 MeV and 2.5 MeV neutron beams. The beam spot size at the target is 10 mm and the neutron rate can be varied between  $10^9$  and  $10^{11}$  n/s, depending on the chosen (DT or DD) neutron source. In the adopted experimental set-up during the neutron irradiation, the GEM detector was placed at about 19 cm from the neutron source, but with the DAQ boards located at one meter. The Ar/CO<sub>2</sub>/CF<sub>4</sub> gas mixture was used because more stable under neutron irradiation at high count rates. The GEM detector was characterized under DD neutron irradiation (2.45 MeV) up to  $2.2 \times 10^6$  n/s, and DT neutron flux (14 MeV) up to  $2.8 \times 10^8$  n/s on the camera (two orders of magnitude higher than DD), equivalent to  $1.2 \times 10^7$  n/s cm<sup>2</sup> on the whole camera. From these tests it was found that the detector response is linear, regardless the gain of the detector, [5]. The detection efficiency of neutron irradiation was estimated to be about  $10^{-4}$  for 2.5 MeV neutrons and  $10^{-5}$  for 14 MeV. The GEM detector response to gamma ray irradiation was measured utilizing a calibrated Co<sup>60</sup> source (gamma rays of energy 1.17 MeV and 1.33 MeV,  $3.8 \times 10^6$  Bq activity). The detection efficiency was found to be of the order of  $10^{-4}$  [5]. Overall, the detection efficiency of the GEM to X-rays is therefore at least three-four orders of magnitude higher than that achieved under gamma and neutrons irradiation, [5].

A scan of gain at a fixed neutron flux ( $1.3 \times 10^6$  n/s) shows that the gamma contribution becomes relevant only at gains greater than 600, while at lower gains (< 400-600) the measured spectrum is given only by neutron conversion. This is confirmed by the comparison with a gain scan when the FNG source is switched off: in this case there are only gammas and they appear for gain higher than 600. X-ray detection in the range 2-20 KeV, typical of present day SXR tomography, requires gain from 100 to 1000. A detailed study performed with scans of threshold, revealed that pulse amplitude distribution is almost flat for neutrons, very peaked at low amplitude for gamma, with changeable derivative as function of gain for X-ray. By means of these different responses to the various radiation sources, discrimination of neutron, gammas and X-rays can be then conceived, playing suitably on the gain and threshold, or by scanning them.

To estimate the energy discrimination capability of the GEM, two targets, Fe and Cu, were combined obtaining a spectrum with two lines. The SXR spectrum was obtained with a Si-PIN diode (AMPTEK XR-100CR, energy resolution of a few percent). The scan of the GEM gain for the Fe and Cu lines shows that it is possible to select an energy region of interest by varying the GEM voltage, at fixed threshold. In particular, by setting  $V_{GEM} = 860$  V the GEM detects 50% of the Cu line (8.2 keV) and 8% of the Fe line (6.4 keV), (Fig. 2a).. In alternative we can use threshold, at fixed gain, to partially discriminate the two lines (Fig. 2b), [7]. This characterization is crucial in order to use the GEM detector as pinhole camera for soft X-ray imaging in tokamak with relevant neutron and gamma yields and with different heating systems, as discussed in a following chapter.

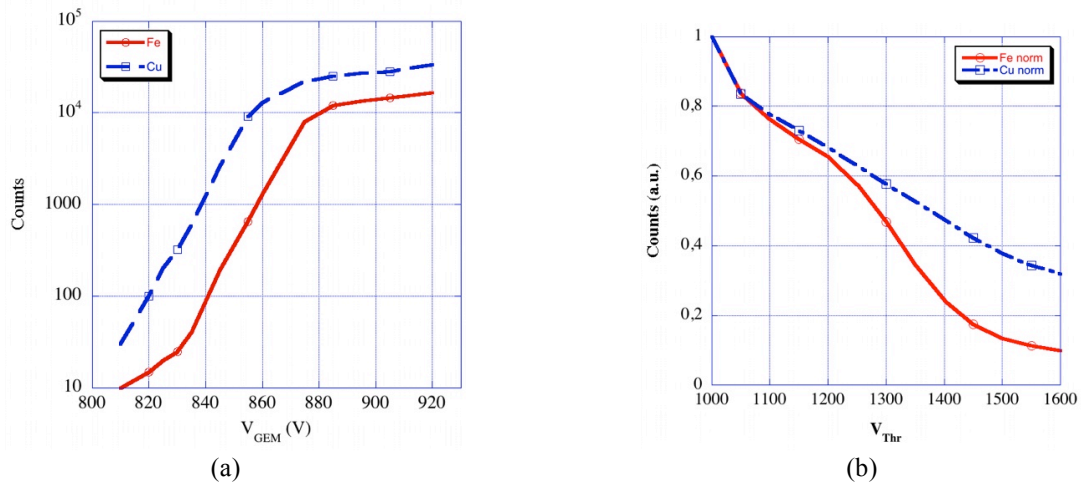


**FIGURE 2.** (a) Comparison of GEM gain scans obtained using the Fe and Cu; (b) Normalized GEM threshold scan for fluorescence spectrum of Fe and Cu.

## POLYCAPILLARY LENSES – LABORATORY CHARACTERISATION

SXR emissions reveal a lot of information about the processes occurring into the magnetic fusion plasmas, but the harsh environmental conditions (including, for example, highly radiative background, high magnetic fields, and often optical limitations) prevent the installation of X-ray detectors directly into, or close to, the machine. To overcome this problem, polycapillary lenses can be used to extract such information for applications in SXR imaging and tomography. Polycapillary lenses offer a large flexibility in designing optical systems, good efficiency and high selectivity for SXR radiation. Tests have been performed in the SXR range (5–25 keV), to characterize the polycapillary lenses for distances much larger than the optical focal length both on the detector and the source sides, [6]. The results from the tests indicate that the polycapillary lenses are energy selective for the X-ray band for which they have been designed. Further, the entrance angle is narrow, making the line of sight very well defined. Polycapillaries offer a large flexibility in designing optical systems to extract SXR radiation from the plasma, transporting it away and they represent therefore a potential tool for both SXR 2-D imaging and tomography in harsh environments.

The polycapillary lenses were characterised in terms of both imaging properties and radiation collection/transport at large distances (up to 7 meters). The half lens was tested by placing a Micro-focus X-ray source (35-80 keV and 0-2 mA, emission spot of about 30  $\mu\text{m}$ ) at its focus input (at  $\sim 4.5$  cm), and using the Medipix as detector at different distances. The spot-sizes acquired at 50 cm and 470 cm are presented in Fig. 3(b) and (c). The output beam was observed to be essentially collimated up to about 5 meters from the source, the divergence measuring approximately 1 mrad, Fig. 3.

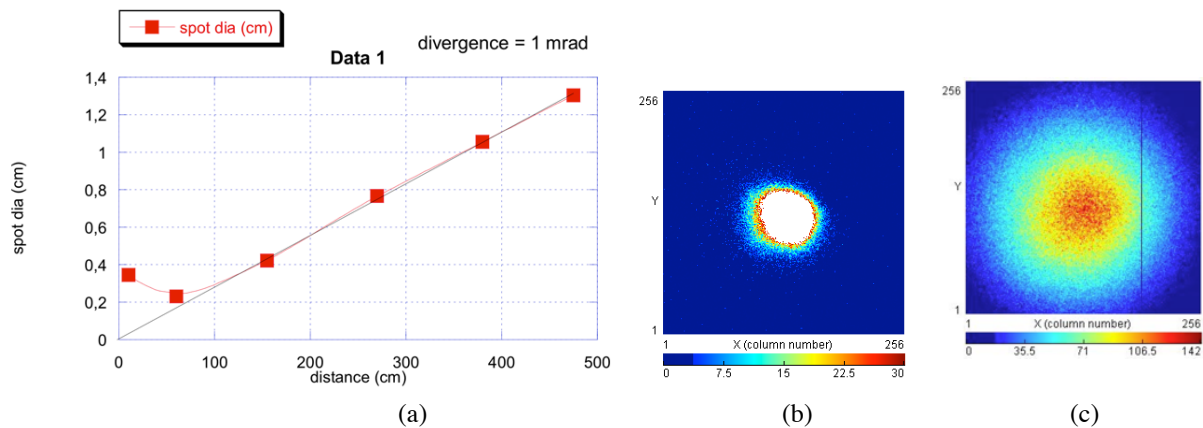


**FIGURE 3.** Experimental characterization of the half lens: (a) divergence measured up to 5 m from the source; (b) spot size at 50 cm; (c) spot size at 470cm from the source.

## C-MOS IMAGERS

The Medipix-2 photon counting chip, developed by INFN at CERN within the Medipix-2 Collaboration, [8] (<http://medipix.web.cern.ch/medipix/pages/medipix2/collaboration.php>) is formed by a square matrix of  $256 \times 256$ ,  $55 \times 55 \mu\text{m}^2$  pixels, resulting in an active area of  $1.4 \times 1.4 \text{ cm}^2$ . Each pixel of the semiconductor sensor (300  $\mu\text{m}$ -thick Si) is bump-bonded to the corresponding channel of the chip (ASIC), providing analog and digital signal processing. The X-Ray photon is converted into the semiconductor and the resulting electric charges are collected at the pixels and transferred to the ASIC. The “USB Interface” is used to connect the Medipix-2 detector to a personal computer. The CMOS chip performs single photon counting in each pixel cell and data are accumulated in a 13-bit counter per pixel, [9]. Thanks to the photon counting mode, it is affected only by shot noise, related to the Poissonian statistic distribution.



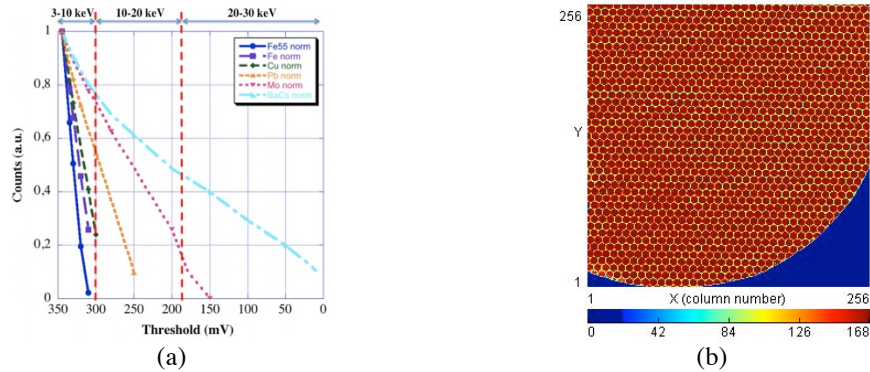


**FIGURE 4.** (a) Normalized threshold scan for different energy spectrum with Medipix-2; (b) Radiography of a GEM foil acquired with Medipix-2.

The Medipix-2 was characterized at ENEA to study its properties at different X-ray energies. The ASIC is equipped with low-threshold discriminators. The adjustable threshold is globally set for all pixels. The energy response of the detector in the X-ray range 0÷30 keV was assessed by scanning the adjustable threshold. The count rate for each pixel is linear up to at least 5 MHz of randomly arriving photons. The read-out time for a full frame is about 10 ms; considering the time needed for data transfer to the computer, a continuous acquisition can be done at about 10 Hz.

The cluster size at different X-ray energies was studied by using the fluorescence lines (Fe, Pb and Mo) and the source of BaCs at low rates and 0.1s acquisition time. Cluster size as a function of energy is constant and equal to 1 for energies up to 6.4 keV, and then it increases linearly up to 2, as expected. The detection efficiency of the Medipix-2 was estimated as a function of photon energy in the range 3÷30 keV, by utilizing an absolutely-calibrated X-ray source (Moxtek 50 kV Bullet) and a spectroscopic Si-PIN diode (AMPTEK XR-100CR). In our experimental set up, SXR line transitions were generated by fluorescence on different samples (KCl, Fe, Cu, Pb, Mo) or by means of radioactive sources of Fe<sup>55</sup> and BaCs. Threshold scans at different energies, in Fig. 4(a), reveal that Fe and Cu lines are not discriminated by the Medipix-2. However, based on these results, three energy bands can still be defined, albeit with a non-negligible overlap: 3÷30 keV (Threshold=345 mV), 10÷30 keV (Threshold=300 mV) and 20÷30 keV (Threshold=180 mV). However, it is possible to operate by subtraction to obtain two completely separated bands (3÷10 keV and 20÷30 keV).

The Medipix-2 imaging capability was tested using the X-ray tube: 10 kV and 10  $\mu$ A. The image of the samples is obtained putting them just in front of the detector to check structure, contrast and spatial resolution. In Fig. 4(b) the image of a GEM foil: the Medipix-2 response is uniform on the whole area without any distortion and the exagonal structure is recognized. At low energy, where the cluster size is 1, the spatial resolution is equal to the pixel dimension (55  $\mu$ m), [9].

The newly acquired PIXIRAD Imaging Counter (<http://pixirad.pi.infn.it>) will be characterized first in the ENEA laboratory, within the next few months, and then, next year, on a tokamak. PIXIRAD Imaging Counters is an INFN-Pisa Spin-off introducing an innovative and high quality X-ray detector with intrinsically and fully digital characteristics. PIXIRAD is based on Chromatic Photon Counting technology and it is able to count individually the incident X-ray photons in the range 2-100 keV and to separate them according to their energy (two color images per exposure). The base of the PIXIRAD is realized by coupling an X-ray sensor made of a thin layer of crystalline CdTe (650  $\mu$ m) to a large area VLSI CMOS pixel ASIC. The CMOS VLSI chip has an active area of 30.7×24.8 mm<sup>2</sup>, organized on a matrix of 512×476 pixels each one of 55×55  $\mu$ m<sup>2</sup>. The sensor is segmented with the same ASIC geometry. The detector is able to count the X-ray photons transmitted through the object and converted in each pixel of the CdTe sensor, in two energy bins.

## EXPERIMENTAL RESULTS OF GEM PINHOLE CAMERA ON KSTAR

The GEM detector built for KSTAR is a compact, portable and flexible detector, fully shielded with a metallic case. The CPU is divided into two parts to perform simultaneously counting without dead time, and data transfer to the computer via Ethernet. Two types of data acquisition systems have been implemented: the first one is sampled at

10  $\mu\text{s}$ , permitting up to 255 frames (acquisitions), but characterized by long dead time for data transfer to the PC after the acquisition. The second system is in continuous mode and permits 60000 frames, sampled at 1ms, but without dead time. The latter DAQ system was developed specifically for KSTAR.

A metallic case was developed to house the detector and the electronic boards, not only for mechanical protection and interface with steerable mechanical mounting on the port, but also for shielding it against electromagnetic and radiofrequency disturbances. The installation on KSTAR, Fig. 5(a), was designed as a pinhole camera, to see most of the core plasma, with adjustable magnification (from  $\times 10$  to  $\times 30$ ). The relative distance of the camera with respect to the port, where the pinhole is mounted, can be adjusted in the range 55–165 cm to achieve the desired magnification, by means of a telescopic tube filled with He to avoid absorption in air, Fig. 5(b). A  $\pm 3.5^\circ$  angular tilt of the camera, pivoted on the pinhole axis, was used to adjust the orientation of the camera (up/down, left/right) when the GEM detector is in the high-magnification configuration. The detector was characterized for two gas mixtures at atmospheric pressure: Ar/CO<sub>2</sub> (70%-30%) and Kr/CO<sub>2</sub> (70%-30%). Specifically, two ranges of operation are available: 3–15 keV with Ar/CO<sub>2</sub> and 3–30 keV with Kr/CO<sub>2</sub>.

In Fig. 6 SXR pictures of the plasma core are shown for different magnifications, in the energy range 3–15 keV. In the right part of the figure, schematic representations of the plasma cross section (in red) and the field of view of the camera (partially transparent blue) at the cross section perpendicular to the optical axes are shown for the different shots, corresponding to different magnification.

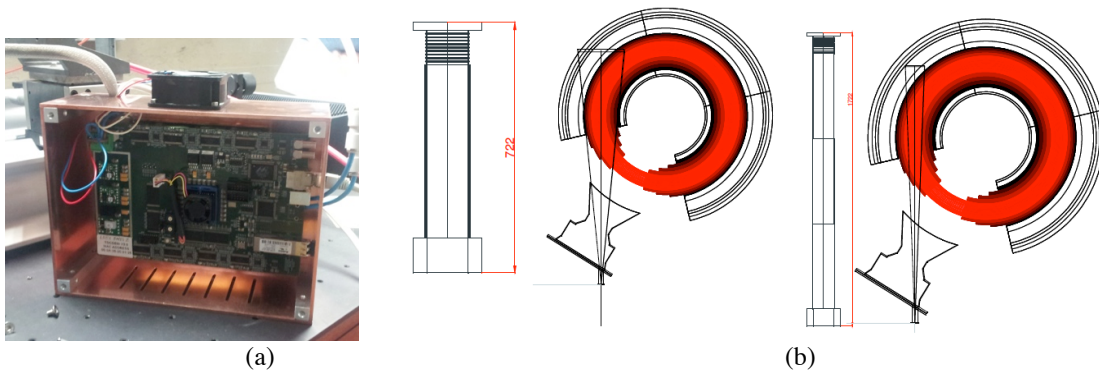


**FIGURE 5.** (a) The FPGA-based motherboard coupled with the GEM detector; (b) Setup at KSTAR (pinhole is located on the port window). Broad view of the plasma (left) and zoomed view (right), together with the length of the tube connecting pinhole to the detector.

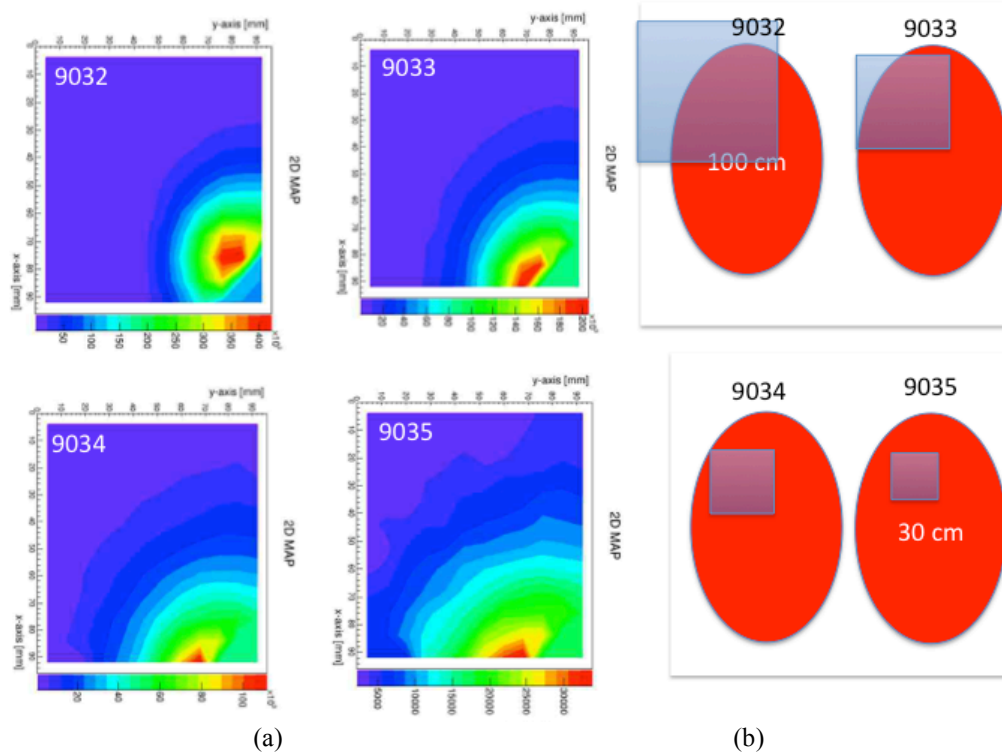


**FIGURE 6.** SXR imaging of the KSTAR plasma core using the GEM system obtained at different magnifications, in the energy range  $3\div 15$  keV: (a) experimental data; (b) corresponding schematic representations of the plasma cross section (red) and the field of view of the camera (partially transparent blue).

When the outer part of the plasma (from the center to the outer edge) is imaged, the pictures, despite the effects of integration along the lines of sight, approximate very well the expected SXR emissivity of the plasma cross section. In shot 9032 the vertical elongation is clearly measurable, while with a progressive zoom, poloidal perturbations of the SXR emissivity curves are well recognizable (shot 9035). The 2D pictures represent the raw data, as acquired in one frame, without any treatment.

In Fig. 7(a) a frame is shown in 3D plot and a contrast (ratio between maximum and minimum values of counts/pixel) of 130 is found. In this case the maximum count rate is 7 MHz/pixel. From the time history of the pixels (Fig. 7(b)) the dynamic range (maximum/minimum count rate), in a shot, was estimated to be larger than 1000. Finally in Fig. 7(c), the time history, with a continuous sampling rate at 1kHz, of a pixel looking at the central peak of the plasma emissivity, is shown and the sawtooth instability is clearly observed.

The total neutron flux on KSTAR for these shots having 2 NBI heating, as estimated from the neutron diagnostics, is about  $10^{14}$  n/s. The neutron background measured with the GEM detector, based on the calibration done at FNG, is  $5 \times 10^7$  n/s  $\text{cm}^2$  (producing about  $2 \times 10^3$  counts/s pixel) and it is coherent with the total neutron yield of KSTAR. The X-ray signal produced in the GEM detector arrives to  $7 \times 10^6$  counts/s pixel, being three-four order of magnitude higher than the neutron background.

In summary, this camera can be considered as a high-performing tomography (high sensitivity, good time resolution, energy discrimination, high dynamic range, noise-free and so on) with 144 lines of sights, organized in a 2D array with imaging capability and optical flexibility (tilting/zooming). Since it works in counting mode, time integration and/or spatial binning can be done post-process with any geometry.

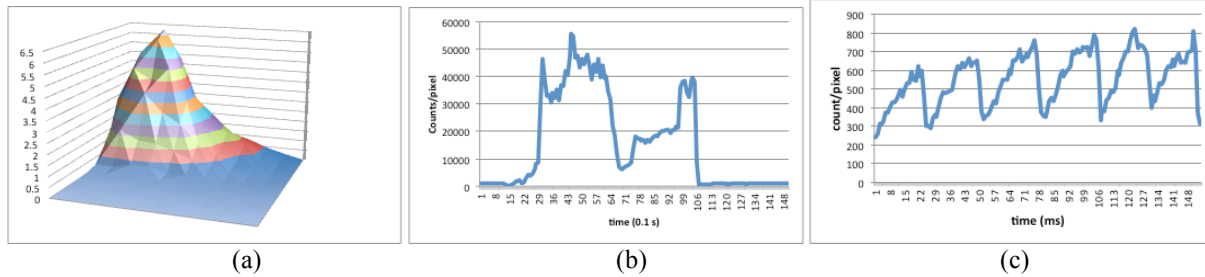


**FIGURE 7.** GEM SXR imaging in KSTAR: (a) 3D plot and contrast ratio of one acquired frame; (b) time history of the pixels, showing the high dynamic range of the system (1000); (c) time history signal of one individual pixel, at a sampling rate of 1kHz, showing sawtooth instability.

## CONCLUSIONS

A new X-ray Laboratory has been established in ENEA-Frascati for SXR diagnostics developments. GEM gas detector confirmed to be flexible, with high performances, robust, pretty insensitive to neutron and gammas, adequate for an “imaging tomography” with “smart” pixels. Polycapillary lenses also seem very promising for transporting soft X-ray radiation at large distances. Medipix could be useful for high definition imaging for soft X-ray to be used far from the plasma. Pixirad is a very performing and powerful C-MOS imager broadband in X-ray and will tested soon. Pixirad and Medipix can be therefore considered complementary to cover the wide X-ray energy range of interest for burning plasma experiments. After this very preliminary and short experimental campaign, all these devices will be fully studied and exploited at KSTAR in the coming years, in a framework of a collaboration ENEA-INFN (Italy) and NFRI-KAIST (South Korea).

## ACKNOWLEDGMENTS

This work was supported by the Euratom Communities under the contract of Association between EURATOM-ENEA. The views and opinions expressed herein do not necessarily reflect those of the European Commission. This research was supported by National R&D Program through the National Research Foundation of Korea (NRF) funded by the Ministry of Science, ICT, of Republic of Korea (No. 2009-0082624).

## REFERENCES

1. D. Pacella et al., Rev. of Sc. Instrum., vol. 72, No. 2 (February 2001)
2. D. Pacella et al., Rev. of Sc. Instrum., vol. 74, No. 3 (March 2003).
3. M. Alfonsi et al., N14-182, IEEE NSS Conference, Puerto Rico (2005).
4. <http://www.fusione.enea.it/LABORATORIES/Tec/FNG.html>
5. D. Pacella et al., Nuclear Instruments and Methods in Physics Research Section A: Accelerators, Spectrometers, Detectors and Associated Equipment, Vol. 720, Pages 53–57, (August 2013)
6. A. Romano et al., 38th EPS Conference on Plasma Physics (2011)
7. D. Pacella et al., 40th EPS Conference on Plasma Physics (2013)
8. X. Llopart et al., IEEE Transact. Nucl. Sci., 49 (5), 2279-2283 (2002)
9. L. Gabellieri et al., 40th EPS Conference on Plasma Physics (2013)